Physical modelling in biomechanics

M. A. R. Koehl

Department of Integrative Biology, University of California, Berkeley, CA 94720-3140, USA
(*cnidaria@socrates.berkeley.edu*)

Physical models, like mathematical models, are useful tools in biomechanical research. Physical models enable investigators to explore parameter space in a way that is not possible using a comparative approach with living organisms: parameters can be varied one at a time to measure the performance consequences of each, while values and combinations not found in nature can be tested. Experiments using physical models in the laboratory or field can circumvent problems posed by uncooperative or endangered organisms. Physical models also permit some aspects of the biomechanical performance of extinct organisms to be measured. Use of properly scaled physical models allows detailed physical measurements to be made for organisms that are too small or fast to be easily studied directly. The process of physical modelling and the advantages and limitations of this approach are illustrated using examples from our research on hydrodynamic forces on sessile organisms, mechanics of hydraulic skeletons, food capture by zooplankton and odour interception by olfactory antennules.

Keywords: scaling; physical models; copepod; antennule; drag; notochord

1. INTRODUCTION

Physical and mathematical modelling are useful techniques in biomechanical research. Both types of models yield quantitative results, permit performance consequences of specific parameters to be investigated in a systematic way not possible using the diversity of organisms available for study, and allow some experiments to be conducted that are not now technically feasible with living organisms. Furthermore, hypotheses about the mechanisms underlying a biomechanical process can be tested using physical or mathematical models. Like mathematical modelling, physical modelling involves simplifying assumptions, thus models that generate predictions that can be tested by comparison with measurements on real organisms are especially useful.

Physical models have long been used in biomechanical research, and many examples are described in textbooks on the subject (Vogel & Wainwright 1969; Vogel & Ewel 1972; Biewener 1992; Vogel 1994). My purpose in this paper is not to review the literature on physical models in biomechanics, but rather to discuss how physical modelling is done and the advantages and limitations of this approach. To accomplish this I will focus mainly on examples taken from our research because I have behind-the-scenes knowledge of the process (and pitfalls) of physical modelling used in these particular studies. I will not stress the details of specific research questions or results of the studies cited, but rather I will use these examples to illustrate a variety of ways in which physical models can be used to enhance biomechanical investigations, and to discuss considerations in the design and scaling of physical models.

2. USEFULNESS OF PHYSICAL MODELS

Physical models enable investigators to explore parameter space in a way that is not possible using the comparative approach with living organisms: parameters can be varied one at a time to quantify the performance consequences of each, while values and combinations not found in nature can be tested. Experiments using physical models in the laboratory or field can circumvent problems posed by uncooperative or endangered organisms. Physical models also permit some aspects of the biomechanical performance of extinct organisms to be measured. Furthermore, use of properly scaled physical models allows detailed physical measurements to be made for organisms that are too small or fast to be easily studied directly.

(a) *Exploring parameter space using physical models*

Quantification of the functional consequences of morphological or behavioural differences between organisms is often helpful in addressing evolutionary or ecological questions. Biomechanics can provide a useful approach for studying the relationship between structure and performance. Although comparison of the morphology and performance of different species in a phylogenetic context can be a powerful way to study adaptations (Wainwright & Reilly 1994), such a comparative approach does not permit a quantitative assessment of the consequences of differences in specific morphological or behavioural parameters. By contrast, mathematical or physical models permit us to measure or calculate defined aspects of performance while holding all morphological or kinematic variables constant except the one(s) we choose to vary. Combinations of morphological and behavioural parameters not available in nature can be tested with physical models so that the consequences of trait interactions can be measured (a statistical approach to quantifying trait

interactions using measurements on physical models is described in Emerson *et al.* (1990)). Physical models can be used to determine whether hypothesized evolutionary changes in morphology, size or behaviour can affect defined aspects of performance (some examples include Chamberlain 1981; Kingsolver & Koehl 1985; Emerson & Koehl 1990; Wootton & Ellington 1991; Koehl 2000). Similarly, physical models permit measurement of the functional consequences of specific traits that are hypothesized to be adaptations to particular types of physical environments (a number of examples are reviewed in Stanley 1988; Rayner & Wootton 1991; Koehl 1996). The results of such experiments can also provide insights for the design of biomimetic devices by elucidating which features of an organism have large or small effects on performance (Mead 2002).

(i) *Example: laboratory study of the effects of morphology on drag*

The first physical models I developed were designed to measure the effects of various features (e.g. shape, orientation, surface texture, mucus coating, flexural stiffness) of marine organisms attached to the substratum on the drag that they experience in ambient water currents (Koehl 1977). Drag is a hydrodynamic force tending to push a body downstream. I was using diverse species of sea anemones, animals with very simple body plans, as the research system to investigate morphological effects on drag, but too many parameters differed between species to permit the hydrodynamic consequences of specific traits to be isolated. However, by measuring the drag on physical models of sea anemones exposed to water currents at a range of velocities in a flume, I was able to assess the consequences of defined changes in a specific parameter, while holding all other features of the model constant. For example, to assess the effects of the crown of feeding tentacles on the drag on a sea anemone, I compared the force on a model body of a given shape and size when it bore no tentacles and when it bore models of tentacular crowns of different shapes, orientations and flexibilities. Such model experiments revealed that most of the drag on an animal was due to drag on its crown, that lobed crowns were subjected to a lower force than solid ones, and that flexible crowns that were able to passively reconfigure into more streamlined shapes as water velocity increased experienced much lower drag than did rigid crowns. Other model experiments enabled me to determine that neither surface bumps (models of the verrucae on sea anemones) nor a mucus coating altered drag in the Reynolds number range at which sea anemones operate. (The Reynolds number, Re, represents the relative importance of inertia to viscosity for a given flow situation; $Re = \rho U L / \mu$, where U is speed, L is a linear dimension such as animal diameter, and ρ and μ are the density and dynamic viscosity, respectively, of the fluid.)

One test of the biological relevance of a physical or mathematical model is comparison of the model output with measurements of the same aspect of performance for the real organisms being modelled. For example, in the case of sea anemones, drag measured on living *Anthopleura xanthogrammica* in the flume were not significantly different from those on models of the same shape, size, flexibility and surface texture (Koehl 1977).

(ii) *Example: field study of effects of seaweed length on forces experienced in waves*

Physical models designed to assess the effects of specific parameters can not only be studied in the laboratory, but also in defined habitats in the field. For example, I measured the effect of thallus length on the peak forces experienced at the holdfasts of models of flexible seaweed blades exposed to waves. Peak forces on models of different lengths could be measured under the same oscillatory flow conditions in a laboratory wave tank (Koehl 1996). By contrast, under messier field conditions, pairs of models of different lengths were attached to force transducers affixed side-by-side to wave-swept rocky shores, and many replicates of such pairs of models were deployed at a variety of sites at which water velocity as a function of time was also recorded (Koehl 1999). In both the laboratory and the field experiments, the model lengths were scaled relative to the distance that the water in the waves moved before reversing direction. Both laboratory and field experiments with physical models showed that, for blade-like floppy organisms that readily move back-and-forth with the flow in waves, once length exceeds the distance the water moves before reversing direction, subsequent growth in length has little effect on peak forces experienced at the holdfast (Koehl 1999, 2000). While the laboratory experiments permitted the mechanisms for this effect to be worked out by simultaneous detailed measurements of flow, force and model displacement in repeatable waves, the field experiments tested whether the same effect of length occurred in the chaotic natural series of waves.

(iii) *Example: effects of shell shape on burrowing by clams*

Physical models can also provide a tool for investigating how morphological features of organisms affect how they interact mechanically with other structures in their environment, such as the substratum, predators or prey. The behaviour of the organisms and of the physical characteristics of the structures with which they interact should be determined for such modelling studies to yield biologically relevant results. For example, robotic models of clams of different shapes were used to assess how the profiles of their shells affect the distance they burrow into the sediment for a fixed number of cycles of burrowing motions (Stanley 1975). When clams burrow, their shells rock back and forth, so a kinematic analysis of ciné films of living clams burrowing had to be conducted so that the robotic clams could be rocked in realistic ways. In addition, the grain sizes of the various sediments tested had to reflect the range of sediment types in which the clams live in nature. The model study revealed that a prosogyrous shell shape (elongate, pointed posterior and rounded, blunt anterior) enhances the ability of a bivalved mollusc to burrow through the sediment by shifting the axis of rotation of the animal anteriorly during the backward phase of shell rotation and posteriorly during the frontward phase of rotation so that the shell 'walks' its way through the sand or mud as it rocks back and forth.

(iv) *Example: effects of fibre reinforcement on the mechanical function of hydraulic skeletons*

Physical models can also be used to address questions about the mechanical support structures of organisms. For

example, effects on the material properties of specific components of composite biomaterials (such as spicules in pliable connective tissues) can be investigated using physical models of the tissues in which the proportions and properties of each component of the material can be varied independently (Koehl 1982). Physical models can also be used to measure the mechanical consequences of specific features of a structure, such as a skeleton. An example of the latter is provided by a study (Koehl *et al.* 2000) of the design of hydraulic skeletons, structures composed of a tension-resisting sheath inflated by fluid under pressure.

During an investigation of how the elongation of an early frog embryo is driven by osmotic swelling of the notochord, which lengthens and straightens as it inflates (Adams *et al.* 1990; Koehl *et al.* 1990), we became curious about which features of an inflating hydraulic skeleton affect its ability to straighten, elongate and push. Many hydraulic structures that inflate osmotically (e.g. notochords, plant cells) or by muscular or ciliary pumps (e.g. echinoderm tube feet, cnidarian polyps) are cylindrical and have tension-resisting walls reinforced by relatively inextensible fibres (e.g. collagen, cellulose). We used physical models (figure 1) to investigate the effects of the orientation of those fibres on several biologically important aspects of the mechanical behaviour of inflating cylindrical hydraulic skeletons: change in shape and size, isometric force production, work done in pulling or pushing, flexural stiffness and resistance to Euler and local buckling (Koehl *et al.* 2000). By using physical models we could keep the uninflated shape of all the skeletons the same, could hold the material properties of the reinforcing fibres and the interfibrillar matrix of the walls of the models constant, and could vary just the fibre angle (θ, the angle of the fibres to the long axis of the cylinder) and the internal pressure.

Experiments using curved models illustrate the type of information such physical modelling can yield (Koehl *et al.* 2000). When inflated, all the models straightened and assumed fibre angles of 54°, regardless of the initial θ value (figure 1). Models with initial values of $\theta < 54°$ widened and increased in flexural stiffness as they straightened, but shortened and thus could pull, but not push. By contrast, models with initial $\theta > 54°$ lengthened and narrowed as they straightened; although they could push, the forces they exerted were limited by their tendency to buckle, which occurred at lower axial loads for models with higher θ values.

Our models of hydraulic skeletons also illustrate some of the limitations of physical models. Although these models could be compared with each other to determine the effects of fibre angle, they could not be used to predict the forces produced by inflating embryonic notochords. The internal pressure of *X. laevis* notochords at different stages of embryonic development has been measured, but the thickness and composition of the sheath change as the embryo develops (Adams *et al.* 1990; Koehl *et al.* 1990) and the resulting material properties of the sheath have not yet been determined. Thus, information necessary to scale the models to be elastically similar to embryonic notochords was unavailable when we fabricated the models. Furthermore, our physical models could not actively
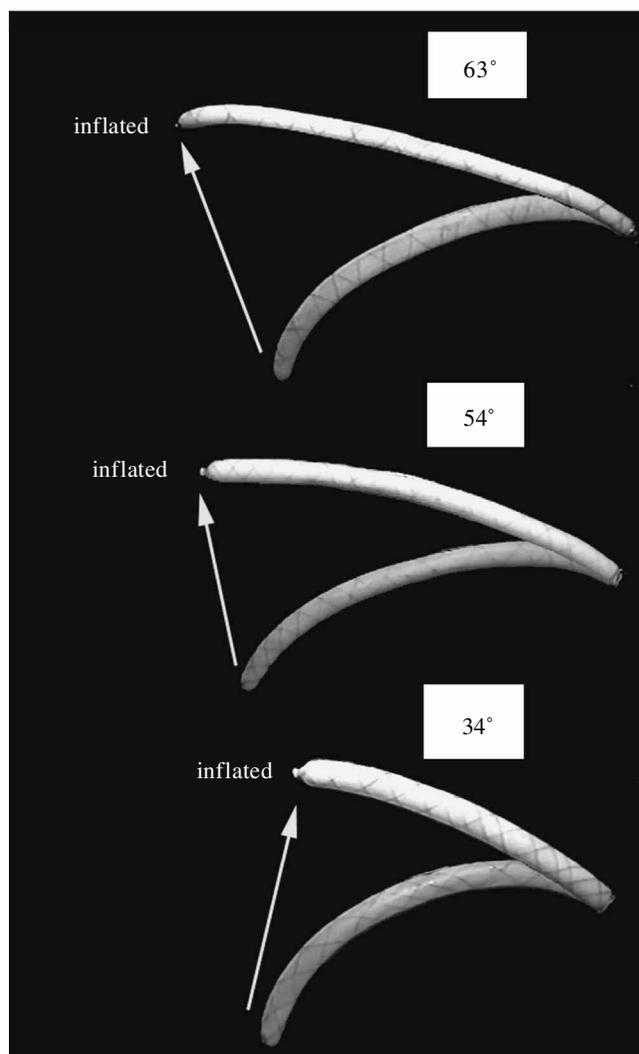

Figure 1. Video images of uninflated (curved) and inflated (straight) physical models of cylindrical hydraulic skeletons. The walls of the models were fabricated from extensible latex reinforced with relatively inextensible nylon fibres in crossed-helical arrays at angles of 63°, 54° and 34° to the long axis of the model (details given in Koehl *et al.* 2000). The curvature of each model before inflation mimicked that of the uninflated notochord of a stage 24 embryo of the frog *Xenopus laevis* (Adams *et al.* 1990). Models were inflated with air to defined pressures, their shape and size changes were measured from video records, and various aspects of the mechanical performance (e.g. flexural stiffness, isometric force production, work performed) were measured as described in Koehl *et al.* (2000). Although all the models straightened upon inflation, those reinforced with fibres at angles greater than 54° elongated, whereas those with angles less than 54° shortened.

grow and remodel during the process of inflation, whereas the sheaths of living embryos do.

(b) *Using physical models to make measuring possible*

Sometimes mechanical measurements can be made using physical models when such measurements are not feasible or are technically difficult for real organisms. For example, some organisms may not behave normally when measuring devices (e.g. force or pressure transducers, strain gauges, thermocouples) are attached to them or

when they are exposed to certain experimental conditions. Furthermore, some species of organisms may be endangered, or may be difficult to collect or to maintain in the laboratory. Physical modelling also provides a mechanism to study the mechanical performance of extinct organisms (Chamberlain 1981, 1991; Kingsolver & Koehl 1985, 1994; Stanley 1988; Briggs *et al.* 1991; Bunker & Machin 1991; Wootton & Ellington 1991). In addition, properly scaled physical models can be used to measure some aspects of the performance of organisms, parts of organisms or the structures they build that either are too small or fast to be measured with precision (Koehl 1995, 1998; Ellington *et al.* 1996; Dickinson *et al.* 1999) or are too large to be studied in the laboratory (Vogel *et al.* 1973).

(i) *Example: sampling of a turbulent odour plume by an olfactory antennule*

The first step in smelling is the capture of odour molecules in the water or air around an organism. We have been studying odour capture by arthropod olfactory antennules. Malacostracan crustaceans, such as lobsters, crabs and stomatopods, flick antennules bearing arrays of aesthetascs (hair-like structures filled with chemosensory neurons; Grünert & Ache 1988; Hallberg *et al.* 1992) through the water (reviewed in Koehl 2001). Odour molecules in marine habitats are carried from sources (such as food or potential mates) by turbulent ambient water currents; malacostracans can track such turbulent odour plumes to their source (reviewed in Weissburg 2000). We used physical models of the spiny lobster, *Panulirus argus*, to study how antennule flicking in turbulent ambient currents affects the temporal and spatial patterns of odour interception by the aesthetascs (Koehl *et al.* 2001).

Physical modelling enabled us to overcome a number of technical difficulties in measuring how flicking antennules interact with turbulent odour plumes (details described in Koehl *et al.* 2001). To compare different manipulations of antennule kinematics or morphology, water flow conditions had to be repeatable between experiments. We conducted our experiments in a flume in which we could control the water flow. However, since the dispersion of odours in the habitats of the lobsters depends on the turbulence as well as the mean velocity of ambient water currents, small-scale flow conditions (ranging from millimetres to centimetres) measured in the field had to be modelled in the flume (figure 2).

Instantaneous fine-scale patterns of odour concentration in a turbulent current are difficult to measure, so we modelled dissolved odour using a fluorescent dye (odour source described in figure 2). An antennule only samples the thin slice of the water column through which it flicks, so we had to sample dye concentrations in the same slice of fluid. We did so by illuminating the dye plume with a sheet of laser light to reveal only the plane through which an antennule swept when it flicked. After calibrating the brightness of pixels in video images to known concentrations of dye in the laser sheet (details in Crimaldi & Koseff 2001), we could use video records of the laser-illuminated slice of the plume to map how dye concentrations in the water evolved with time during our experiments. This PLIF technique showed that a plume that looked like a diffuse cloud was actually made up of
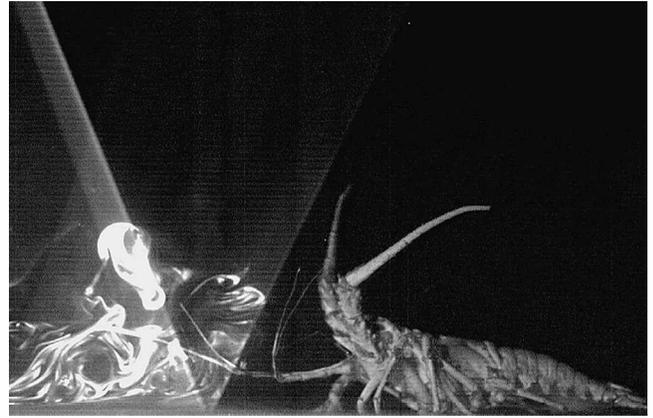

Figure 2. Video image of a model of the spiny lobster, *Panulirus argus*, in a flume (details given in Koehl *et al.* 2001). The small-scale turbulence of the water flow in the flume was designed to replicate turbulence measured using acoustic Doppler velocimetry at similar heights above the substratum in shallow coral reef habitats (M. A. R. Koehl, unpublished data). Fluorescent dye (Rhodamine 6G), which we used as an analogue of a dissolved odour, was pumped at $0.05\ \text{ml s}^{-1}$ through a porous foam outlet flush with the floor of the flume to model a source (e.g. food) leaching odour into the environment. Flow in this image was moving from left to right at a mean freestream velocity of $10\ \text{cm s}^{-1}$, and the model lobster was 1 m downstream from the dye source. The model lobster was made from the molted exoskeleton of a *P. argus*. Fresh antennules from real *P. argus* were mounted on the model and flicked by a computer-controlled motor to mimic the kinematics of *P. argus* antennules (Goldman & Koehl 2001). A laser sheet illuminated just the plane of the dye plume through which the antennule flicked (in this image, the laser sheet is shining down in front of the lobster from the top of the tank and is reflected up towards the left corner of the image by a mirror on the floor of the tank). The whole model is shown in this figure, but high-speed (250 fps) close-up videos of just the aesthetasc-bearing region of the antennules (field imaged = 3.62 cm × 3.16 cm) were digitized, and the brightness of each pixel in each image was used to determine instantaneous dye concentration in the plume and within the aesthetasc array.

fine filaments of high concentration swirling in clean water (figure 2). Although dye concentrations measured at a point downstream from a source fluctuated rapidly with time (Koehl *et al.* 2001), the statistical descriptions of concentration distributions in turbulent plumes changed with distance from the source (Crimaldi & Koseff 2001). Thus, dye encounters by antennules during large numbers of replicate flicks had to be measured to characterize the consequences to odour sampling of differences in parameters such as antennule velocity or hair arrangement. Unfortunately, it is difficult to convince a lobster to repeatedly flick an antennule in the plane of laser light at a defined distance from the dye source. We overcame this problem using a mechanical model of a *P. argus* to flick fresh antennules from real *P. argus* at specific positions in the sheet of laser light (figure 2). We programmed the model lobster to mimic the flicking kinematics measured for antennules of living *P. argus* (Goldman & Koehl 2001). By digitizing high-speed close-up video images of the aesthetasc-bearing region of an antennule flicked by the model lobster, the fine-scale spatial and temporal patterns of dye concentrations in the plume and in the array of

aesthetascs could be measured (details in Koehl *et al.* 2001).

Our experiments with models of lobsters and odour plumes revealed that water penetrates the aesthetasc array on an antennule during the fast downstroke of the flick, carrying fine-scale patterns of concentration into the receptor area. This spatial pattern, blurred by flow along the antennule during the downstroke, is retained during the slower return stroke and is not shed until the next flick. Thus, physical models enabled us to learn that flicking antennules take discrete samples in space and time of the pattern of concentrations in an odour plume. Although these experiments with models showed how antennules hydrodynamically alter the patterns of concentration arriving in the aesthetasc array, they did not reveal which aspects of these patterns are used by the lobsters to navigate in an odour plume. Living lobsters must be used to determine which spatial or temporal aspects of these concentration patterns affect the firing of neurons in the olfactory pathway, and which correlate with behavioural choices made by animals during odour-plume tracking.

Physical models that fail can also reveal important features of the system being studied. For example, in a study in which we used a mechanical lobster to flick real antennules in an odour plume (M. A. R. Koehl, B. A. Best and P. A. Moore, unpublished data), we put a chemical marker (dopamine) in the plume in our flume, and we mounted a small dopamine-sensing probe (Moore *et al.* 1989) within the aesthetasc array of each antennule tested. By comparing the time course of dopamine concentrations encountered by the probe when the antennule was flicking versus stationary, we hoped to determine the effect of flicking on odour interception. The model experiment failed because we rarely got any signals from the probe (never when it was still, and only once in a while when it flicked). This opened our eyes to the importance of monitoring odour interception along the length of the whole antennule rather than at a point because turbulent odour plumes are full of aroma-free holes, and led to the modelling studies using the PLIF technique described in this section.

3. DESIGN OF PHYSICAL MODELS

Just as theoreticians must specify the assumptions of their mathematical models, experimentalists need to clarify that the structural features and mechanical properties of their physical models represent some of the assumptions underlying their investigations. For example, fabrication of rigid ceramic models of sea anemones whose drag is to be measured is based on the simplifying assumptions that these animals do not deform when exposed to hydrodynamic forces and that they do not secrete mucus. Such assumptions should be tested whenever possible. One way to test whether model assumptions are realistic is to compare the assumed features of a physical model with measurements of such features for living organisms. For example, videos of living sea anemones exposed to water currents like those to be employed in the model experiments can be used to test the assumption that these animals are rigid. Another way to evaluate the assumptions underlying the design of a physical model is to manipulate an assumed feature and to determine the mag-

nitude of the effects of the manipulation on the performance variables to be assessed in the model study. For instance, measurements of drag on flexible model sea anemones and on mucus-coated models can be compared with those on the rigid, mucus-free models (Koehl 1977).

An important aspect of the design of physical models that are not the same size as the prototype organism is the scaling of the models such that the aspect(s) of performance to be investigated are preserved. For example, if momentum exchange between an appendage and the surrounding fluid is important, the model appendage should be dynamically similar to the prototype, whereas if oxygen transport to the appendage surface is critical, then the relative importance of bulk fluid flow to molecular diffusion should be the same for the model as for the real organism. If branch sagging under self-weight relative to branch length is the critical aspect of performance to be assessed, then model trees should be elastically similar to the prototypes, whereas if trunk breakage by wind is of interest, then models should have safety factors (maximum stress experienced due to aerodynamic forces on the tree relative to breaking strength of the trunk tissues) similar to those of the species being modelled. Models of walking and running animals should operate at the same Froude number as the locomoting animals. Biological texts about organism size and allometry, as well as engineering texts about fluid mechanics or structural design, can provide useful information about dimensionless indices that must be maintained for proper scaling of different types of functions. Often it is impossible to properly scale all aspects of performance simultaneously; hence compromises between the various aspects of function to be modelled must be made based on knowledge of the ecology and physiology of the organisms and on the questions being addressed by the experiments.

(a) *Dynamically scaled physical models*

Perhaps the most familiar sort of scaling for model experiments in biomechanics is the use of dynamically scaled physical models to study flow velocities and forces on organisms or parts of organisms locomoting through fluids or experiencing ambient water flow or wind (described in Vogel 1994). If a model is geometrically similar to the prototype organism or structure and if it operates at the same Reynolds number (*Re*), then the relative importance of inertia and viscosity in determining flow patterns and forces on the body will be the same for the model as for the prototype. If a model and the prototype are dynamically similar, then the ratios of the velocities and of the forces at comparable positions in the flow field around the model and the real organism are the same. For example, if the velocity at a position located one body length upstream of a fish's nose is twice as big as the velocity at a point three body lengths downstream of its tail, then the velocity one model length upstream of the nose of a dynamically similar model is double that of the velocity three model lengths downstream of its tail.

Sometimes dynamically scaled models are used to make measurements in a fluid that is technically more convenient than the one in which the living organism functions. For example, flow visualizations are easier to do in water than in air because water is denser than air. Finding neutrally buoyant dyes or particles for use in water is sim-

ple, whereas producing neutrally buoyant bubbles or making smoke filaments without causing heat-induced air convection for flow tracking in air is challenging. For this reason, we visualized flow patterns around the wings of dynamically scaled model insects in water rather than in air (Kingsolver & Koehl 1985). Similarly, Vogel studied the role of flow-induced pressures in a variety of aquatic organisms (squid, Vogel 1987; scallops, Vogel 1985) using dynamically scaled models in a wind tunnel because '...it just happened that [he] had equipment for measuring very low pressures only in air' (Vogel 1994, p. 103).

Flow and force measurements can generally be made with greater signal-to-noise ratios for large models than for microscopic organisms. As $Re = \rho UL/\mu$, the Re of a microscopic organism swimming in water can be maintained for a large model (L) moving more slowly (U) in another Newtonian fluid with a higher viscosity (μ). One important challenge in using large physical models of microscopic organisms is that bodies moving at low Re influence fluid movement many body-lengths away from themselves (Vogel 1994). Therefore, the walls of the tank in which low-Re models are tested can influence the flow and forces on the models (Loudon *et al.* 1994). For this reason, tanks must be very large relative to the models (e.g. we use a cubic metre tank of mineral oil for experiments on models that are a few centimetres in length of flapping appendages that operate at Re numbers of order 1–100). Furthermore, controls must be run in tanks of different sizes to measure wall effects (Loudon *et al.* 1994), and walls near which low-Re appendages operate (such as the body surface or substratum) should be incorporated in physical models of such structures.

(i) *Example: hydrodynamics of copepod feeding appendages*

Many types of aquatic animals use appendages composed of rows of hair-like structures (e.g. setae) to catch particulate food, such as unicellular organisms, suspended in the surrounding water. Calanoid copepods are abundant planktonic crustaceans (body length of a few millimetres); many species feed on single-celled algae and form a critical link in aquatic food webs (reviewed in Koehl 1984). We have been using diverse copepods to investigate the physical mechanisms by which setulose appendages capture food particles. Copepods catch algal cells using a pair of appendages, the second maxillae (M2s), which they fling apart from each other and squeeze back together (Koehl & Strickler 1981). The coarseness of the mesh of hairs on the M2s varies between species, as does the speed at which they move; hence the Re values of the setae on copepod M2s (calculated using seta diameter for L) range from 10^{-2} to 1 (Koehl 1995). Mathematical (Cheer & Koehl 1987) and physical (Hansen & Tiselius 1992; Leonard 1992; Loudon *et al.* 1994; Koehl 1995) models of fluid movement around and through arrays of cylinders revealed that this Re range is a critical one in which the flow of fluid through the array changes drastically: only a small proportion of the fluid encountering a row of cylinders at $Re = 10^{-2}$ flows through the gaps between cylinders, whereas a large fraction of the fluid moves between adjacent hairs at $Re = 1$.

We have been studying the hydrodynamic mechanisms by which the fling-and-squeeze motions by a pair of setulose appendages capture particles in this transitional Re
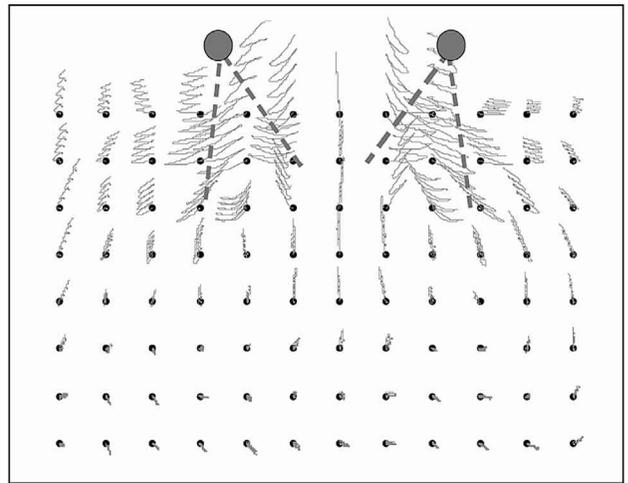

Figure 3. Paths of fluid movement near models of the second maxillae (M2s) of a calanoid copepod, *Eucalanus pileatus*. The M2 models, which were constructed of steel wire and aluminium, were geometrically similar to the M2 models of *E. pileatus*. Neither the prototype M2s nor the models bent when flapping through the fluid. In the example illustrated here, the model M2s were programmed to execute repeated fling-and-squeeze motions that swept through the same arc and were dynamically similar to the M2 motions of *E. pileatus* when feeding on small (4 μm) algal cells (M. A. R. Koehl and G.-A. Paffenhöfer, unpublished data). The large grey circles indicate the drive rods rotating the M2 models, which were mounted at a plate (not drawn in the diagram) that represented the ventral surface of the animal. The long axis of the animal being modelled would be at right angles to the page and its mouth would be located medially between the M2 hinges. The dashed lines represent the positions of the M2s at the extremes of the arcs through which they swept, flinging apart from and squeezing back towards each other. The small black dots represent the positions of the midpoints of parcels of fluid at the beginning of the experiment (for clarity, only a few of the points in our sampling grid are shown). The fine grey lines represent the paths of fluid during five consecutive cycles of fling-and-squeeze by the model M2s. Instantaneous velocity vector fields were determined using the particle image velocimetry technique described by Cowen & Monismith (1997). These vectors were used to determine the new positions of the parcels of fluid at the next time step, and so on. This experiment showed that such motions by the M2s pump fluid towards the mouth of the animal (M. A. R. Koehl and T. Cooper, unpublished data).

range, and how they are affected by appendage morphology and kinematics. Although diverse copepods provide a range of morphologies and Re values to study, making detailed measurements of water movement around and through microscopic hairs whose motions last only 10–30 ms is difficult. For this reason, as well as the need to explore combinations of parameters not available in nature, we used a modelling approach to address this question. As the three-dimensional geometry and time-varying kinematics of copepod M2s relative to each other and the body surface are complex, we used dynamically scaled physical models rather than mathematical models to study copepod feeding mechanisms. Details of model design and operation are given in Koehl (1995) and in figure 3.

Even complex physical models differ from real organisms, so it is important to examine the assumptions underlying physical models. For example, in constructing our models of copepod M2s, we assumed that the body surface was flat, and that the copepod's other appendages did not have an important effect on flow produced by the M2s. We tested these assumptions by determining that the relative water velocities during mid-fling near real copepod M2s (measured by tracking small particles in the water recorded in high-speed, high-magnification ciné films of feeding copepods; G.-A. Paffenhöfer and M. A. R. Koehl, unpublished data) were not significantly different from those measured at comparable positions near the model M2s (M. A. R. Koehl and J. Jed, unpublished data).

Our model experiments revealed that M2s whose setae operate at $Re \sim 1$ function like leaky sieves that capture particles by filtering them from the water passing through the M2s during the squeeze. By contrast, we found that M2s whose setae operate at $Re \sim 10^{-2}$ capture algal cells by creating water currents that carry these particles towards the mouth (Koehl 1995, 1998). Our model experiments also showed that different morphological and kinematic parameters affect hydrodynamic performance of setulose appendages at $Re \leqslant 10^{-2}$ than at higher Re (Koehl 1996, 2000).

(b) *Conflicting scaling requirements*

In some situations, scaling physical models to preserve one type of function precludes scaling them correctly for another aspect of performance. When this occurs, either choices have to be made about which aspects of model performance can be compromised, differently scaled models of the same structure can be used to study different functions, or mathematical and physical modelling can be done in conjunction with each other.

(i) *Example: combining mathematical and physical modelling to study odour capture by antennules*

Stomatopods ('mantis shrimp') are malacostracan crustaceans that have a simple (and thus easily modelled) arrangement of aesthetascs on their olfactory antennules. We used stomatopods to study how the kinematic and morphological changes that occur during the ontogeny and growth of olfactory antennules (Mead *et al.* 1999) affect the flux of odour molecules to the surfaces of the aesthetascs during antennule flicking. To scale momentum exchange between the antennule and the water so that we could use physical models to determine the water velocity vector fields through the aesthetasc array, we used models that had the same Re values as the real antennules (Mead & Koehl 2000). However, to scale the mass exchange between the water and the aesthetacscs, our models should have had the same Péclet number as the prototype antennules. (The Péclet number, Pe, reflects the importance of convection relative to diffusion in transporting fluid-borne molecules; $Pe = UL/D$, where D is the diffusion coefficient of the molecule of interest in the fluid.). Unfortunately, when using large models of microscopic structures, it is not practical to scale both Re and Pe simultaneously. The way that we resolved this dilemma was to use physical modelling to determine the detailed velocity vector fields around the aesthetascs (Mead & Koehl 2000) and to measure the concentration distri-

butions in the filaments of odour in a turbulent plume (Koehl *et al.* 2001). We then used mathematical modelling to calculate the diffusion of molecules in such odour filaments as they were carried by our measured velocity field through the aesthetasc array (Stacey *et al.* 2002). This combination of mathematical and physical modelling enabled us to predict the flux of molecules to the chemosensory aesthetascs as a function of time, and thus to determine the effects of morphological and kinematic parameters of antennules on factors that affect the firing of olfactory neurons, such as the onset slope and peak flux of odour molecules to receptors (Stacey *et al.* 2002).

4. CONCLUSIONS: WHY USE PHYSICAL MODELS?

Many of the same research goals can be accomplished by mathematical and by physical modelling. However, there are a number of situations in which physical models offer some useful advantages. For example, when complex three-dimensional structures using non-steady-state kinematics are being studied, construction of a physical model can be a faster process than development of a complex computer simulation. Another tangible advantage of physical modelling is that handling the models (literally feeling the forces on them and experiencing their behaviour) can enhance our intuitive understanding of biomechanical processes and provide insights about underlying mechanisms. For this reason, physical models can also be effective tools for teaching biomechanics. Furthermore, physical models can be used by biologists who lack the mathematical training or computer skills necessary to develop mathematical models.

REFERENCES

Adams, D. S., Keller, R. E. & Koehl, M. A. R. 1990 Mechanism of straightening and elongation of the notochord of *Xenopus laevis*. *Development* **110**, 115–130.

Biewener, A. A. (ed.) 1992 *Biomechanics, structures and systems: a practical approach*. Oxford: IRL Press.

Briggs, D. E. G., Dalingwater, J. E. & Selden, P. A. 1991 Biomechanics of locomotion in fossil arthropods. In *Biomechanics in evolution* (ed. J. M. V. Rayner & R. J. Wootton), pp. 37–56. Cambridge University Press.

Bunker, S. J. & Machin, K. E. 1991 The hydrodynamics of cephalaspids. In *Biomechanics in evolution* (ed. J. M. V. Rayner & R. J. Wootton), pp. 113–129. Cambridge University Press.

Chamberlain Jr, J. A. 1981 Hydromechanical design of fossil cephalopods. In *The Ammonoidea* (ed. M. R. House & J. R. Senior), pp. 289–336. London: Academic.

Chamberlain Jr, J. A. 1991 Cephalopod locomotor design and evolution: the constraints of jet propulsion. In *Biomechanics in evolution* (ed. J. M. V. Rayner & R. J. Wootton), pp. 57–98. Cambridge University Press.

Cheer, A. Y. L. & Koehl, M. A. R. 1987 Paddles and rakes: fluid flow through bristled appendages of small organisms. *J. Theor. Biol.* **129**, 17–39.

Cowen, E. A. & Monismith, S. G. 1997 A hybrid digital particle tracking velocimetry technique. *Exp. Fluids* **22**, 199–211.

Crimaldi, J. P. & Koseff, J. R. 2001 High-resolution measurements of the spatial and temporal scalar structure of a turbulent plume. *Exp. Fluids* **31**, 90–102.

Dickinson, M. H., Lehmann, F.-O. & Sane, S. P. 1999 Wing rotation and the aerodynamic basis of insect flight. *Science* **284**, 1954–1960.

Ellington, C. P., Van Den Berg, C., Willmott, A. P. & Thomas, A. L. 1996 Leading-edge vortices in insect flight. *Nature* **384**, 626–630.

Emerson, S. B. & Koehl, M. A. R. 1990 The interaction of behavioral and morphological change in the evolution of a novel locomotor type: 'flying' frogs. *Evolution* **44**, 1931–1946.

Emerson, S. B., Travis, J. & Koehl, M. A. R. 1990 Functional complexes and additivity in performance: a test case with 'flying' frogs. *Evolution* **44**, 2153–2157.

Goldman, J. A. & Koehl, M. A. R. 2001 Fluid dynamic design of lobster olfactory organs: high-speed kinematic analysis of antennule flicking by *Panulirus argus*. *Chem. Senses* **26**, 385–398.

Grünert, U. & Ache, B. W. 1988 Ultrastructure of the aesthetasc (olfactory) sensilla of the spiny lobster, *Panulirus argus*. *Cell Tissue Res.* **251**, 95–103.

Hallberg, E., Johansson, K. U. I. & Elofsson, R. 1992 The aesthetasc concept: structural variations of putative olfactory receptor cell complexes in crustaceans. *Microsc. Res. Techn.* **22**, 325–335.

Hansen, B. & Tiselius, P. 1992 Flow through the feeding structures of suspension feeding zooplankton: a physical model approach. *J. Plankton Res.* **14**, 821–834.

Kingsolver, J. G. & Koehl, M. A. R. 1985 Aerodynamics, thermoregulation, and the evolution of insect wings: differential scaling and evolutionary change. *Evolution* **39**, 488–504.

Kingsolver, J. G. & Koehl, M. A. R. 1994 Selective factors in the evolution of insect wings. *A. Rev. Entomol.* **39**, 425–451.

Koehl, M. A. R. 1977 Effects of sea anemones on the flow forces they encounter. *J. Exp. Biol.* **69**, 87–105.

Koehl, M. A. R. 1982 Mechanical design of spicule-reinforced connective tissues: stiffness. *J. Exp. Biol.* **98**, 239–268.

Koehl, M. A. R. 1984 Mechanisms of particle capture by copepods at low Reynolds numbers: possible modes of selective feeding. In *Trophic dynamics within aquatic ecosystems* (ed. D. G. Meyers & J. R. Strickler), pp. 135–166. Boulder, CO: Westview Press.

Koehl, M. A. R. 1995 Fluid flow through hair-bearing appendages: feeding, smelling, and swimming at low and intermediate Reynolds number. *Soc. Exp. Biol. Symp.* **49**, 157–182.

Koehl, M. A. R. 1996 When does morphology matter? *A. Rev. Ecol. Syst.* **27**, 501–542.

Koehl, M. A. R. 1998 Small-scale hydrodynamics of feeding appendages of marine animals. *Oceanography* **11**, 10–12.

Koehl, M. A. R. 1999 Ecological biomechanics: life history, mechanical design, and temporal patterns of mechanical stress. *J. Exp. Biol.* **202**, 3469–3476.

Koehl, M. A. R. 2000 Consequences of size change during ontogeny and evolution. In *Scaling in biology* (ed. J. H. Brown & G. B. West), pp. 67–86. New York: Oxford University Press.

Koehl, M. A. R. 2001 Fluid dynamics of animal appendages that capture molecules: arthropod olfactory antennae. In *Computational modeling in biological fluid dynamics*, vol. 124 (ed. L. J. Fauci & S. Gueron), pp. 97–116. New York: Springer.

Koehl, M. A. R. & Strickler, J. R. 1981 Copepod feeding currents: food capture at low Reynolds number. *Limnol. Oceanogr.* **26**, 1062–1073.

Koehl, M. A. R., Adams, D. S. & Keller, R. E. 1990 Mechanical development of the notochord in early tail-bud amphibian embryos. In *Biomechanics of active movement and deformation of cells* (ed. N. Akkas), pp. 471–485. Berlin: Springer.

Koehl, M. A. R., Quillin, K. J. & Pell, C. A. 2000 Mechanical design of fiber-wound hydraulic skeletons: the stiffening and straightening of embryonic notochords. *Am. Zool.* **40**, 28–41.

Koehl, M. A. R., Koseff, J. R., Crimaldi, J. P., McCay, M. G., Cooper, T., Wiley, M. B. & Moore, P. A. 2001 Lobster sniffing: antennule design and hydrodynamic filtering of information in an odor plume. *Science* **294**, 1948–1951.

Leonard, A. B. P. 1992 *The biomechanics, autecology and behavior of suspension-feeding in crinoid echinoderms*. San Diego, LA: University of California.

Loudon, C., Best, B. A. & Koehl, M. A. R. 1994 When does motion relative to neighboring surfaces alter the flow through an array of hairs? *J. Exp. Biol.* **193**, 233–254.

Mead, K. S. 2002 Using lobster noses to inspire robot sensor design. *Trends Biotechnol.* **20**, 276–277. (DOI 10.1016/S0167-7799(02)01979-0.)

Mead, K. S. & Koehl, M. A. R. 2000 Stomatopod antennule design: the asymmetry, sampling efficiency, and ontogeny of olfactory flicking. *J. Exp. Biol.* **203**, 3795–3808.

Mead, K. S., Koehl, M. A. R. & O'Donnell, M. J. 1999 Stomatopod sniffing: the scaling of chemosensory sensillae and flicking behavior with body size. *J. Exp. Mar. Biol. Ecol.* **241**, 235–261.

Moore, P. A., Gerhardt, G. A. & Atema, J. 1989 High resolution spatio-temporal analysis of aquatic chemical signals using microelectrochemical electrodes. *Chem. Senses* **14**, 829–840.

Rayner, J. M. V. & Wootton, R. J. (eds) 1991 *Biomechanics in evolution*. Cambridge University Press.

Stacey, M. T., Mead, K. S. & Koehl, M. A. R. 2002 Molecule capture by olfactory antennules: mantis shrimp. *J. Math. Biol.* **44**, 1–30.

Stanley, S. M. 1975 Why clams have the shape they have: an experimental analysis of burrowing. *Paleobiology* **1**, 48–58.

Stanley, S. M. 1988 Adaptive morphology of the shell in bivalves and gastropods. In *The Mollusca*, vol. 11. *Form and function* (ed. E. Trueman & M. Clarke), pp. 105–141. New York: Academic.

Vogel, S. 1985 Flow-assisted shell reopening in swimming scallops. *Biol. Bull.* **169**, 624–630.

Vogel, S. 1987 Flow-assisted mantle cavity refilling in squid. *Biol. Bull.* **172**, 61–68.

Vogel, S. 1994 *Life in moving fluids*. Princeton University Press.

Vogel, S. & Ewel, K. C. 1972 *A model menagerie*. Reading, MA: Addison-Wesley.

Vogel, S. & Wainwright, S. A. 1969 *A model menagerie*. Reading, MA: Addison-Wesley.

Vogel, S., Ellington, C. P. & Kilgore Jr, D. C. 1973 Wind-induced ventilation of the burrow of the prarie dog, *Cynomys ludovicianus*. *J. Comp. Physiol.* **85**, 1–14.

Wainwright, P. C. & Reilly, S. M. (eds) 1994 *Ecological morphology: integrative organismal biology*. University of Chicago Press.

Weissburg, M. J. 2000 The fluid dynamical context of chemosensory behavior. *Biol. Bull.* **198**, 188–202.

Wootton, R. J. & Ellington, C. P. 1991 Biomechanics and the origin of insect flight. In *Biomechanics in evolution* (ed. J. M. V. Rayner & R. J. Wootton), pp. 99–112. Cambridge University Press.

GLOSSARY

PLIF: planar laser-induced fluorescence